Report 2005 - 05
July

Calorimetric Low Temperature Detectors for Heavy Ion Physics

P. Egelhof and S. Kraft-Bermuth

(accepted for publication in: Cryogenic Particle Detection, Topics Appl. Phys. 99 (2005),
Chr. Enss (Ed.), Springer-Verlag Berlin Heidelberg 2005)

Gesellschaft für Schwerionenforschung mbH
Planckstraße 1 · D-64291 Darmstadt · Germany
Postfach 11 05 52 · D-64220 Darmstadt · Germany

Calorimetric Low Temperature Detectors for Heavy Ion Physics

P. Egelhof[1,2] and S. Kraft-Bermuth[1,2]

[1] Gesellschaft für Schwerionenforschung, Planckstrasse 1, D 64291 Darmstadt, Germany
[2] Institut für Physik, Johannes Gutenberg Universität Mainz, Staudingerweg 7, D 55128 Mainz, Germany

Abstract. Calorimetric low temperature detectors have the potential to become powerful tools for applications in many fields of heavy ion physics. A brief overview of heavy ion physics at present and at the next generation heavy ion facilities is given with a special emphasis on the conditions for heavy ion detection and the potential advantage of cryogenic detectors for applications in heavy ion physics.

Two types of calorimetric low temperature detectors for the detection of energetic heavy ions have been developed and their response to the impact of heavy ions was investigated systematically for a wide range of energies ($E = 0.1$–360 MeV/amu) and ion species (^{4}He ... ^{238}U). Excellent results with respect to energy resolution, $\Delta E/E$ ranging from 1 to 5×10^{-3} even for the heaviest ions, and other basic detector properties such as energy linearity with no indication of a pulse height defect, energy threshold, detection efficiency and radiation hardness have been obtained, representing a considerable improvement as compared to conventional heavy ion detectors based on ionization. With the achieved performance, calorimetric low temperature detectors bear a large potential for applications in various fields of basic and applied heavy ion research. A brief overview of a few prominent examples, such as high resolution nuclear spectroscopy, high resolution nuclear mass determination, which may be favourably used for identification of superheavy elements or in direct reaction experiments with radioactive beams, as well as background discrimination in accelerator mass spectrometry, is given, and first results are presented. For instance, the use of cryogenic detectors allowed to improve the sensitivity in trace analysis of ^{236}U by one order of magnitude and to determine the up to date smallest isotope ratio of $^{236}\mathrm{U}/^{238}\mathrm{U} = 6.1 \times 10^{-12}$ in a sample of natural uranium.

Besides the detection of heavy ions, the concept of cryogenic detectors also provides considerable advantage for X-ray spectroscopy in atomic physics with highly charged heavy ions. Such detectors are to be used in near future for sensitive tests of quantum electrodynamics in very strong electromagnetic fields by a precise determination of the 1s Lamb shift in hydrogen-like heavy ions. The status of development of a high-resolution and highly efficient detector for hard X-rays is reported, the performance of which is with $\Delta E/E = 1.1 \times 10^{-3}$ for $E_\gamma = 60$ keV close to fulfill the demands of the Lamb shift experiment.

1 Introduction

The success of experimental physics and the quality of experimentally determined results generally depend on the quality of the available detection

systems with respect to energy resolution, detection threshold, detection efficiency, granularity, etc. Consequently, the search for improved detection techniques is always a basic part of research activities in all disciplines of physics. When focusing on atomic, nuclear, particle and astrophysics, detectors for radiation – covering photons from the visible light via X-rays to hard γ-rays, and particles such as α- or β-radiation, light and heavy ions in a wide range of energies, and various exotic particles – will be important.

Whereas most of the standard methods for detection of radiation are based on ionization, the concept of cryogenic detectors, where photons or particles are detected independent of ionization processes, opens completely new and promising perspectives for radiation detectors. A large variety of detection concepts for cryogenic detectors has been investigated over the years by numerous research groups all over the world for many applications in different fields of physics, and excellent results have been reported [1,2]. Attempts to develop cryogenic detectors for applications in heavy ion physics were started about 15 years ago at the University of Mainz, Germany, and at GSI Darmstadt, Germany, and have meanwhile succeeded to obtain interesting and promising results, which have recently lead to first applications in experiments. The aim of the present contribution is to give an overview of heavy ion physics with a special emphasis on the potential applications of cryogenic detectors and the requirements for such detection schemes, to discuss the status of the development and the performance of such detectors for a number of topics of interest, and to present the first results which have been achieved.

An overview of the heavy ion facilities, presently existing and planned for the future project FAIR, at GSI Darmstadt, which is chosen exemplarily as one of the leading centers for heavy ion physics worldwide, is displayed in Fig. 1 (for details see [3,4]). Some of the specialities of that facility (at present and in the future) are, among many others:

- the production and acceleration of intense beams of all ion species from hydrogen to uranium with a wide range of kinetic energies starting around the Coulomb barrier ($E \approx 3$–10 MeV/amu) up to relativistic energies ($E \approx$ 100–2000 MeV/amu) or even higher at the future facility FAIR;
- the production of isotopically clean intense beams of radioactive ions by in-flight separation in the fragment separators FRS and SFRS, and their use for nuclear structure and nuclear astrophysics investigations on nuclei located far outside the valley of stability in the chart of nuclides;
- the storage of stable as well as radioactive ion beams in storage rings and their cooling to highest phase space densities, then reaching excellent beam qualities with energy spreads of $\Delta E/E \leq 10^{-4} - 10^{-6}$;
- the separation, detection and unique identification of very rare isotopes, such as, e.g., in the search for superheavy elements [5,6] (with event rates down to ≤ 1/week), and in accelerator mass spectrometry [7,8] where small isotope ratios down to 10^{-16} are to be measured;

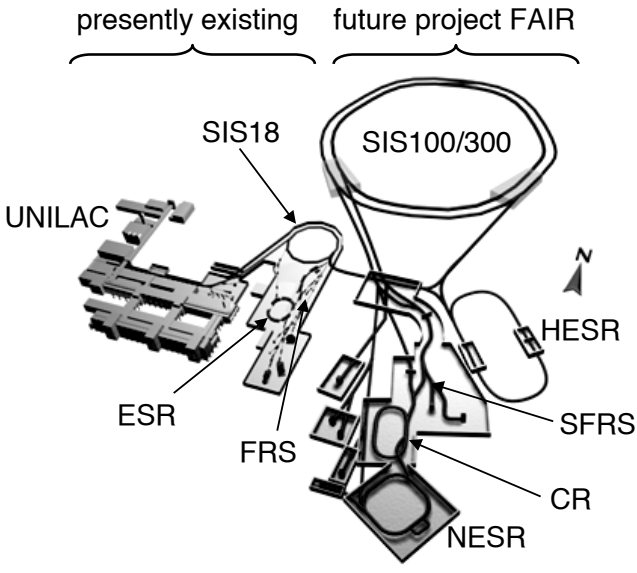

Fig. 1. Schematic view of the existing GSI facility *(left)* with the linear accelerator UNILAC, the heavy ion synchrotron SIS18, the fragment separator FRS and the experimental storage ring ESR, and the future project FAIR *(right)* with the double ring synchroton SIS100/300, the high energy antiproton storage ring HESR, the superconducting fragment separator SFRS, the collector ring CR and the new experimental storage ring NESR.

– the production and storage of highly charged, bare or hydrogen- and helium-like very heavy ions and their use for atomic physics experiments.

As compared to the present GSI facilities, the performance at the future facility FAIR will improve the experimental conditions with respect to beam intensities, luminosities and variety of potential applications by orders of magnitude. With such or similar performance at the GSI facilities as well as at the present and future facilities worldwide, extended physics programs addressing a wide spectrum of physics questions are currently running or will be started in near future. As will be discussed below in more detail, for some future investigations of considerable interest, detectors with highest energy resolution and/or highest detection efficiency and low detection threshold are required, reaching a performance not obtained with conventional detection systems currently available. For example, heavy ion detectors with an energy resolution of the order of $\Delta E/E \leq 10^{-3}$ are required:

– for high-resolution nuclear spectroscopy with cooled heavy ion beams available from storage rings;
– for mass identification via combined energy/time-of-flight detection for reaction products in direct reaction and γ-spectroscopy experiments with

radioactive beams. Such experiments, performed in inverse kinematics, require an event by event identification of the beam-like reaction products [4];
- for a unique, background-free and highly efficient mass determination, again via combined energy/time-of-flight techniques, for the identification of superheavy elements;
- for a highly efficient and background-free identification of rare isotopes in accelerator mass spectrometry [7,8] via a high-resolution total energy measurement. Hereby, high detection efficiency for very slow heavy ions ($E \leq 0.1$ MeV/amu) is also very important.

Whereas conventional heavy ion detectors, such as semiconductor detectors and ionization chambers, which operate on a charge collection principle, provide relative energy resolutions for the heaviest ions of only about $\Delta E/E \geq (1-5) \times 10^{-2}$, and have relatively high detection thresholds for slow very heavy ions, the concept of cryogenic detectors promises, due to its different operation principle, considerable advantage over conventional detectors with respect to energy resolution, detection efficiency, energy threshold and radiation hardness. High-resolution magnet spectrographs are capable of achieving a relative resolution as good as 10^{-3} or better, but at the cost of very limited solid angle and thus detection efficiency, and charge state ambiguities, especially for slow heavy ions.

Besides heavy ion detectors, also photon detectors are important for heavy ion physics. Highly charged stored heavy ions, interacting with an internal target, provide a source of characteristic hard X-rays ($E \leq 100$ keV) which need to be detected with highest energy resolution, not reached by conventional semiconductor detectors, to obtain the necessary spectroscopic information for sensitive tests of **Q**uantum **E**lectro**D**ynamics (QED) and other topics of interest in atomic physics [4,9,10].

In summary, it turns out that cryogenic detectors for heavy ions and hard X-rays have the potential to be powerful tools for atomic and nuclear physics experiments at heavy ion accelerators, and are worth to be considered and further developed in the future.

The present contribution is organized in the following way: After experimental conditions in heavy ion physics and requirements for cryogenic heavy ion detectors are considered in Sect. 2, detector design and detector performance will be discussed in Sect. 3. Section 4 contains examples for potential applications and first results on experiments with cryogenic detectors in heavy ion physics. In Sect. 5 layout and performance of detectors for hard X-rays, which are applied in atomic physics experiments with highly charged heavy ions, are discussed.

2 Experimental Conditions and Specific Requirements for Cryogenic Heavy Ion Detectors

When constructing cryogenic detectors for energetic heavy ions, it has to be realized that the conditions and detector parameters with respect to absorber size, incident energy, energy resolution, amount of radiation damage, etc., are different by orders of magnitude from those of most other applications of such detectors [1,2]. As already discussed in Sect. 1, the typical incident kinetic energies of the heavy ions to be detected in the various applications range from energies well below the Coulomb barrier ($E \leq 0.1$–1 MeV/amu) via energies around the Coulomb barrier ($E \approx 3$–10 MeV/amu) up to relativistic energies ($E \geq 100$–2000 MeV/amu), thus corresponding to total energies of $E \approx 10$–20 MeV up to some hundred GeV. Despite the relatively large total energies, the high specific energy loss of heavy ions in matter leads to comparably small ranges (2 μm–15 mm in most cases, except for light relativistic ions, see also Table 1), thus allowing relatively small absorber volumes. If quantitatively compared to the case of photons, electrons or protons, etc., it turns out that, due to the characteristic energy loss processes, the energy deposit per range in matter is for heavy ions by orders of magnitude higher. This specific feature makes calorimetric low temperature detectors, which reach their highest sensitivities for small absorber sizes, attractive for the detection of heavy ions. Due to the relatively high incident energies, already operating temperatures around 1.5 K will allow sufficient sensitivity of calorimetric detectors for heavy ions, thus reducing the demands on low temperature technology.

Table 1. Range of various heavy ions in sapphire for energies between 0.1 and 500 MeV/amu (calculated using the program TRIM [11]).

E (MeV/amu)	Range (μm) for			
	^{20}Ne	^{40}Ar	^{132}Xe	^{238}U
0.1	1.4	1.6	2.7	2.7
1	6	7	10	12
10	94	72	57	62
100	4760	2980	1230	945
500	70820	43780	15920	8080

After having fixed the conditions for heavy ion detection, we may address the question of what can be the potential advantages of cryogenic detectors for heavy ions, and where are the limitations. Due to their operation principle

the potential advantage of calorimetric low temperature detectors over conventional ionization detectors – such as semiconductor detectors or ionization chambers, etc. – are:

- the smaller energy gap ω for the creation of an elementary excitation, leading to a better counting statistics: Whereas the energy gap for producing an electron-ion pair in a conventional semiconductor detector is of the order of a few eV, the excitation energy of thermal phonons is of the order of $\omega \leq 10^{-3}-10^{-4}$ eV. This results in a potentially better energy resolution and lower energy threshold, both decreasing with $\sqrt{\omega}$. It should be noted, however, that for the relatively large incident energies of heavy ions this effect is of minor importance, except for the lowest total energies of $E \leq 10$ MeV;
- the more complete energy detection: For ionization detectors, considerable losses in the ionization signal up to 60–80% appear due to direct phonon creation and charge recombination (the latter effect is especially dominating for very heavy ions due to the extremely high charge densities) and result in a substantial pulse height defect. In contrast, for calorimetric detectors principally the whole deposited energy, besides small losses (see below), is finally transferred into heat after the decay of the initial electronic excitations;
- the lower detection threshold due to the absence of dead layers and entrance windows, which are unavoidable in conventional ionization detectors and therefore result, especially for very slow heavy ions, in limitations in detection efficiency and energy resolution due to energy loss straggling effects;
- the flexibility in the choice of the absorber material: As compared to semiconductor detectors, a much wider variety of materials is expected to fulfill the conditions for absorber materials of calorimetric detectors. The absorber material may therefore be optimized with respect to radiation hardness and other criteria. The short lifetimes caused by radiation damage, mainly due to lattice damage by nuclear stopping, are one of the basic limitations of semiconductor detectors when detecting high count rates of very heavy ions.

The fundamental limit on the energy resolution of a calorimetric detector is given by thermodynamic fluctuations of the energy content in the absorber (also called phonon noise) and the Johnson noise of the thermistor [12,13]. For the detectors discussed in Sect. 3, these contributions are as low as 10–100 keV. An overview of practical limitations of energy resolution due to various effects is given in [13]. For the special case of cryogenic heavy ion detection, where the slowing down and stopping mechanisms considerably affect the lattice structure of the absorber, we expect that the limit of intrinsic resolution will be determined by the solid state properties of the absorber material. Theoretical predicitions for the energy resolution of cryogenic detectors for some selected cases of ion species and absorber material are given

in [14,15]. It is found that statistical fluctuations of that amount of energy, which finally does not contribute to the thermal signal, will determine the intrinsic limit of energy resolution. Such loss processes are due to the creation of local lattice defects, so-called "Frenkel pairs" which give rise to phonon trapping, the creation of long living metastable electronic states with lifetimes much longer than the thermal time constant of the detector, the stored energy consequently not contributing to the thermal signal, the creation of photons which escape from the absorber volume, etc. Unfortunately, there is presently not much known about the quantitative contribution of these effects to the energy resolution. For the special case of calorimetric detection of 25 MeV Br ions in a diamond absorber, a relative energy resolution of $\Delta E/E = 2.5 \times 10^{-3}$ is predicted in [14]. Qualitatively it is expected that the effects discussed above contribute most for very slow and very heavy ions for which nuclear stopping is dominant, whereas for faster ions ($E \geq$ 0.1–0.2 MeV/amu) electronic stopping contributes most to the specific energy loss (see also [11,15]).

For the future, systematic investigation of the energy resolution of calorimetric low temperature detectors for various ion species, incident energies and absorber materials may provide more quantitative information, not only on properties of the detectors, but, vice versa, also on the solid state properties of the absorber materials (see also Sect. 3).

3 Design and Performance of Calorimetric Low Temperature Detectors for Energetic Heavy Ions

The principles of cryogenic detectors, based on semiconductor thermistors as well as on **T**ransition **E**dge **S**ensors (TES), are discussed in detail in the contributions by *Mc Cammon* and *Irwin et al.*, respectively, to this volume [16,17]. We shall therefore not repeat this discussion, but focus in this section on the technical details and realization of such detectors for the special case of detection of energetic heavy ions.

3.1 Detector Design

Within the last 15 years, two types of calorimetric detectors for heavy ions with different thermometers, one on the basis of a semiconducting germanium thermistor, and the other on the basis of a superconducting phase transition thermometer, have been developed. A detailed discussion of the layout and the preparation of these detectors may be found in [15,18–24].

3.1.1 Calorimetric Detectors Based on Semiconductor Thermistors

The first type of calorimeter is prepared on the basis of a germanium thermistor. It consists of a $3 \times 1 \times 0.5$ mm^3 germanium crystal, heavily doped

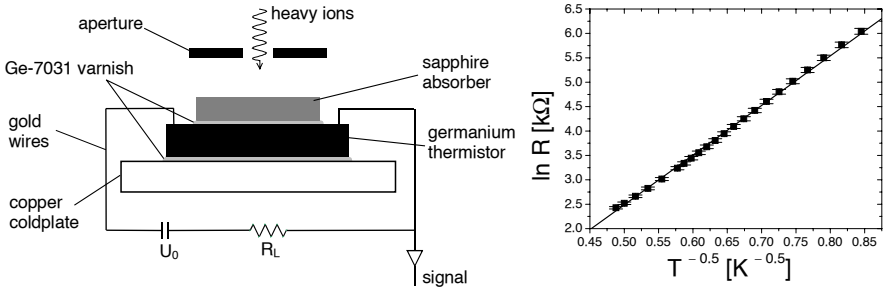

Fig. 2. The setup of a calorimetric heavy ion detector with a semiconducting germanium thermistor is schematically displayed on the *left side* (for details see text). The corresponding *R(T)* characteristics is shown on the *right side*. The *solid line* represents a fit to the data using the modified Mott equation [17].

and compensated with indium (2×10^{17} atoms/cm^3) and antimony (1×10^{17} atoms/cm^3). For such compensated semiconductors, conduction is realized mainly by the so-called "phonon assisted hopping conductivity" [17]. Consequently, the *R(T)* characteristics is well described by the modified Mott equation $R(T) = R_0 \exp(T_0/T)^{1/2}$ with the parameters $R_0 = 69\ \Omega$ and $T_0 = 106$ K (see solid line in Fig. 2, right side), determined by the semiconductors material properties. At a typical operating temperature around $T = 1.7$ K, the resistance is $R = 200\ \mathrm{k}\Omega$ with a $\mathrm{d}R/\mathrm{d}T = -0.48\ \mathrm{M}\Omega/\mathrm{K}$, corresponding to a thermistor sensitivity $\alpha = (1/R)(\mathrm{d}R/\mathrm{d}T) = -2.4\ \mathrm{K}^{-1}$.

A schematic view of the detector setup is displayed in Fig. 2 (left side). The germanium crystal is glued onto a copper coldplate with GE-7031 varnish. The electrical contacts are realized by thermal pressure bonding with gold wires of 25 µm in diameter. As absorber a sapphire crystal ($2 \times 1 \times 0.33$ mm^3) is glued with GE-7031 varnish onto the germanium thermistor. Sapphire is a suitable absorber material because of its low heat capacity, the Debye temperature amounting to $\Theta_D = 1025$ K. The thermistor is biased by a battery through a load resistor ($R_L = 10\ \mathrm{M}\Omega$). The voltage signal due to the impact of an incident ion is read out by conventional pulse electronics, namely a voltage sensitive preamplifier (bandwidth: 1 kHz–10 kHz, gain: 1000–10 000) and a shaping amplifier (shaping time: 25–200 µs).

To adapt such detectors to very low ion energies, detectors with smaller heat capacities were also developed. For these detectors, the germanium thermistor has dimensions of only $0.5 \times 0.5 \times 0.5$ mm^3 and the sapphire absorber of $3 \times 3 \times 0.05$ mm^3, respectively. With this setup, the heat capacity and also the thermal coupling to the heat sink are reduced by about one order of magnitude, thus allowing higher sensitivity for low energetic heavy ions [15].

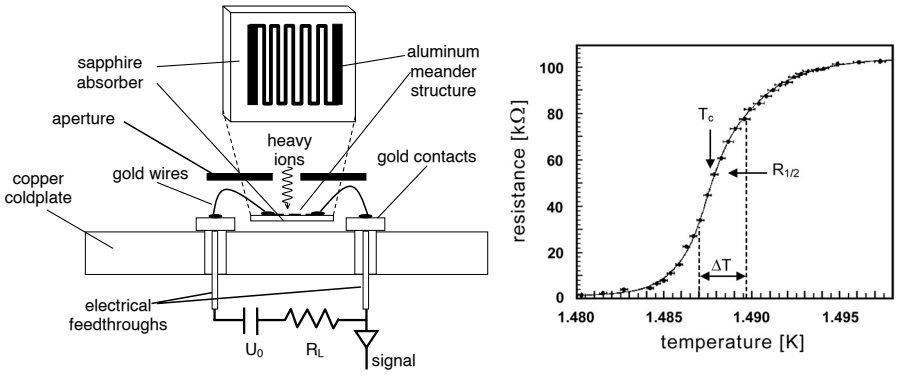

Fig. 3. The setup of a calorimetric heavy ion detector with a superconducting aluminum TES calorimeter is schematically displayed on the *left side*. The corresponding *R(T)* characteristics is shown on the *right side* (for details see text).

3.1.2 Calorimetric Detectors Based on Aluminum Transition Edge Sensors

The second type of calorimeter consists of a superconducting thin aluminum film, which is operated in the region of the phase transition between the super- and the normalconducting state, and again a sapphire absorber. The setup, shown schematically in Fig. 3 (left side), is similar to the one for the germanium calorimeter (Fig. 2), the main difference being that the aluminum thermistor is evaporated as a thin film on the surface of the sapphire substrate. The thickness of the aluminum film of about 10 nm is adjusted to provide a narrow transition width for high sensitivity. In order to match the resistance of the microstrip to conventional preamplifiers, the aluminum film is patterned in a meander-like structure by photolithographic techniques[1]. It consists of 51 connected strips of 10 μm width and 1 mm length each [21]. A typical observed *R(T)* characteristics is displayed in Fig. 3 (right side). The phase transition appears at a temperature of $T_c = 1.488$ K with a width of $\Delta T = 2.9$ mK and an impedance of $R(T_c) = 52$ kΩ, yielding a sensitivity of $\alpha(T_c) = (1/R)(\mathrm{d}R/\mathrm{d}T) = 404\ \mathrm{K}^{-1}$. In contrast to the germanium calorimeters discussed above, the detectors with aluminum thermistors are not glued onto the copper coldplate, but supported only by the gold wires of 25 μm diameter, which realize the electrical contact.

For both types of calorimeters the absorber thickness is adjusted to the individual experimental conditions. Especially for the case of relativistic heavy ions where the standard absorber thickness of 330 μm is not sufficient to stop the ions, additional sapphire absorbers are glued onto the sapphire substrate.

[1] Photolithography is provided by K. Haberle et al., Institut für Halbleitertechnik, Technische Universität Darmstadt, Schlossgartenstrasse 8, D 64289 Darmstadt, Germany.

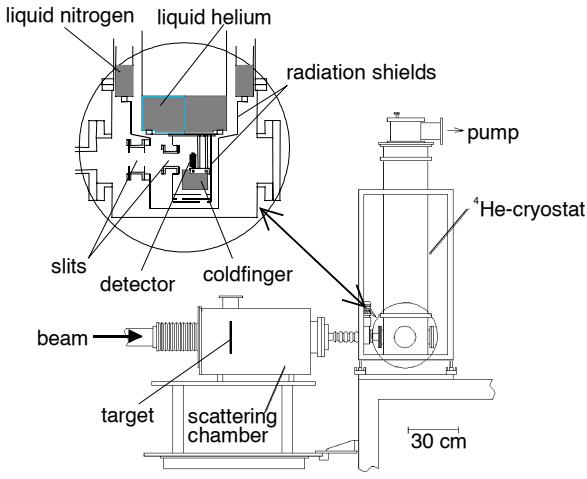

Fig. 4. Schematic view of the experimental setup for heavy ion detection (for details see text).

These detectors are fixed by specially shaped copper support structures in order to minimize thermal contact to the environment.

3.2 Detector Performance

In several measurements, the detectors discussed in the previous section were tested with various heavy ion beams (^{13}C ... ^{238}U) at various energies ranging from 0.1 MeV/amu up to 360 MeV/amu, and their response to the impact of heavy ions and their performance were systematically investigated. For both types of detectors excellent results have been obtained. In the following, a brief overview of the most prominent results is given (for a more detailed discussion see [15,18–25]).

Whereas measurements at higher energies (E = 5–360 MeV/amu) were done at GSI with heavy ion beams from the UNILAC accelerator and from the synchrotron SIS18 (see Fig. 1), experiments at lower energies (E = 0.1–1 MeV/amu) were performed at the VERA facility located at the university of Vienna, Austria [26]. The experimental setup used for most of the measurements is shown in Fig. 4. A pumped ^{4}He window cryostat, operated at temperatures between 1.2 K and 4.2 K, is used to cool down the detectors to their operating temperature. The detectors are mounted on a cold finger (see insert in Fig. 4) which is temperature regulated by an electronic control circuit. A temperature stability of about 10 μK was achieved in the earlier measurements. With recent improvements in temperature regulation, a temperature stability of $\leq$ 1 μK is reached (see [15] for details). To improve the

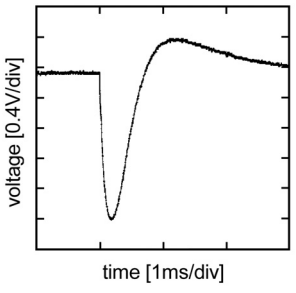

Fig. 5. Preamplifier signal due to the impact of a 11.4 MeV/amu ^{136}Xe ion onto the germanium calorimeter.

performance, a new cryostat was designed recently, especially adjusted to the needs of heavy ion research, providing considerably higher cooling power and allowing for a larger detector solid angle. For the measurements, the cryostat is connected to a scattering chamber or directly to the beamline at one of the accelerator facilities discussed above. Both scattering chamber and cryostat, are mounted on a movable arm, allowing the detectors to be irradiated either by Rutherford-scattered ions from thin target foils, or by the direct beam at reduced intensity.

In Fig. 5, a preamplifier signal for the impact of a 11.4 MeV/amu ^{136}Xe ion onto the germanium calorimeter is displayed. From the observed pulse height a temperature rise of the calorimeter of $\Delta T = 9.5$ mK at an operating temperature of $T = 1.7$ K was obtained. The decay time of about

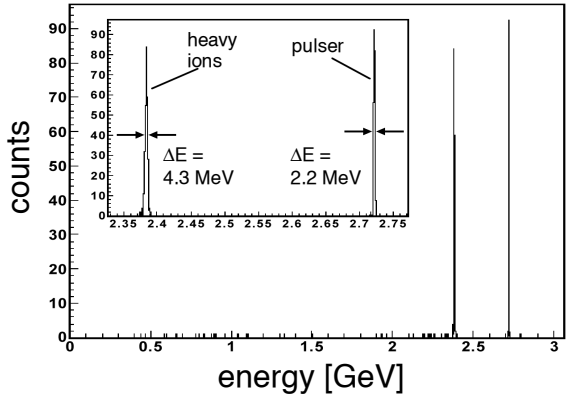

Fig. 6. Energy spectrum obtained with the germanium calorimeter for 11.6 MeV/amu ^{209}Bi ions. The *insert* shows the peaks due to the heavy ions and due to a pulser on an expanded scale. The relative energy resolution achieved is $\Delta E/E = 1.8 \times 10^{-3}$.

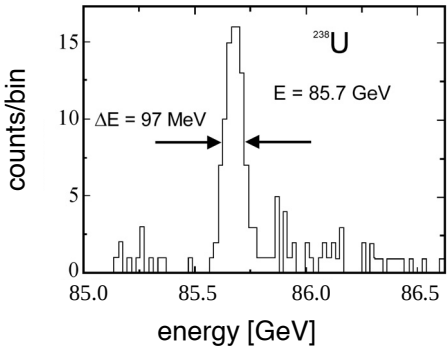

Fig. 7. Energy spectrum obtained with the aluminum TES calorimeter for a cooled ^{238}U beam with $E = 360$ MeV/amu which was extracted from the ESR storage ring at GSI Darmstadt. The obtained relative energy resolution is $\Delta E/E = 1.1 \times 10^{-3}$.

$\tau = 250$ µs is determined by the thermal coupling to the heat sink and allows for count rates up to about 0.5–1 kHz. An energy spectrum for 11.6 MeV/amu ^{209}Bi ions, again taken with the germanium calorimeter [19], is displayed in Fig. 6. The baseline noise was determined with a pulser, which was coupled to the preamplifier, to be $\Delta E = 2.2$ MeV. For the incident ^{209}Bi ions a clean spectrum showing a narrow Gaussian peak with a width of $\Delta E = 4.3$ MeV was obtained, which corresponds to a relative energy resolution of $\Delta E/E = 1.8 \times 10^{-3}$. This result already represents a considerable improvement as compared to conventional ionization detectors, in particular for such very heavy ions. For the detectors with aluminum transition edge sensors similar results were obtained [20–23]. For example, for 4.8 MeV/amu ^{58}Ni ions an energy resolution of $\Delta E/E = 1.6 \times 10^{-3}$ was achieved.

In further test measurements the detectors were also irradiated with relativistic heavy ions, provided from the heavy ion synchrotron SIS18 (see Fig. 1). For 100 MeV/amu ^{20}Ne ions a relative energy resolution of 1.9×10^{-3} was obtained [23] (see also Fig. 11), again representing for these high energies a considerable improvement as compared to conventional detectors. Of special interest was a comparison, where data were taken [22] with two detectors of the same type, but with different absorber sizes ($V = 6$ mm^3 and $V = 121$ mm^3). In spite of the large difference in heat capacity, the energy resolution obtained was comparable. This indicates that the resolution in this case was not limited by the sensitivity of the detector, and provides perspectives for the design of large solid angle detector systems.

When summarizing all the results obtained at energies above $E = 5$ MeV/amu, it turns out that the relative energy resolutions of $(1.6–1.9) \times 10^{-3}$ are very similar, independent on the ion species, the ion energy, the type of detector and the absorber size. These findings indicate that the present limitation in energy resolution is not determined by the intrinsic detector resolution due to sensitivity, thermal or electronic noise contributions, heat capacity, statistics of the energy loss processes, etc. (see Sect. 2), but most probably by the quality of the heavy ion beams from the UNILAC and SIS18 accelerators, namely the energy spread of these beams, which is expected

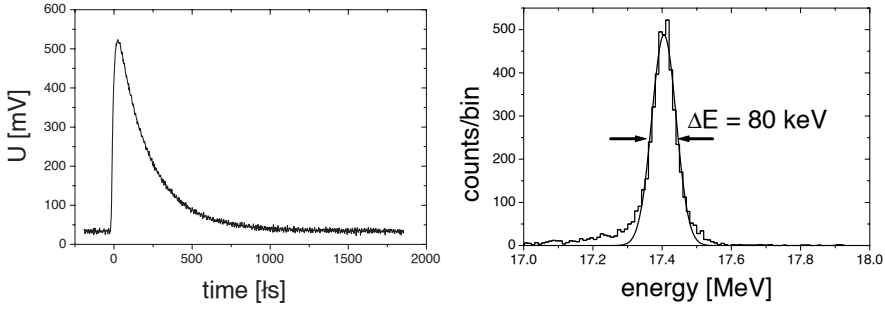

Fig. 8. Preamplifier signal *(left side)* and energy spectrum *(right side)* for ^{238}U ions at $E = 17.39$ MeV obtained with the aluminum TES calorimeter. The relative energy resolution achieved is $\Delta E/E = 4.6 \times 10^{-3}$.

to be of the order of $\Delta E/E \approx (1-2) \times 10^{-3}$. Consequently, in one further experiment [23] the detectors were tested with a cooled heavy ion beam, extracted from the storage ring ESR (see Fig. 1). The energy spread of the beam was determined from Schottky spectra of the circulating beam to be better than $\Delta E/E = 2.4 \times 10^{-4}$. The resulting energy spectrum, obtained for the aluminum TES calorimeter, is displayed in Fig. 7. For a 360 MeV/amu ^{238}U beam a relative energy resolution of $\Delta E/E = 1.1 \times 10^{-3}$ was achieved, which represents the up to date best result for heavy ions.

For some potential applications (see Sect. 4), high resolution detectors for relatively low ion energies of $E \leq 1$ MeV/amu are needed. Therefore, the response of calorimetric detectors to the impact of very low energetic heavy ions was recently studied [15] using ^{13}C, ^{197}Au and ^{238}U beams at various incident energies ranging from total energies of $E = 10$ MeV to $E = 60$ MeV, corresponding to $0.1 \leq E \leq 1$ MeV/amu. In addition, data for 5.5 MeV α-particles provided by a ^{239}Pu/^{241}Am/^{244}Cm source, mounted inside the cryostat, were taken. As the lowest energy provided by the UNILAC accelerator at GSI is around 3 MeV/amu, these investigations were performed at the 3 MV Tandem accelerator of the VERA facility at the university of Vienna, Austria [26]. This facility is discussed in detail in Sect. 4.3, where also the experimental arrangement is displayed in Fig. 17. The present measurements took advantage of the excellent beam qualities provided by this facility, the energy spread being of the order of $\Delta E/E \leq 10^{-4}$, and the fact that changing from one ion species to another is a fast and relatively easy operation which facilitates systematic investigations with various ion species at various energies.

All measurements were performed with the aluminum TES calorimeters, because these detectors provide higher sensitivities for low energies as compared to the germanium calorimeters (see Sect. 3.1). A preamplifier signal for the impact of a ^{238}U ion with $E = 17.39$ MeV is displayed in Fig. 8 (left side). The relatively short thermal decay time of $\tau = 206$ µs allows for count rates

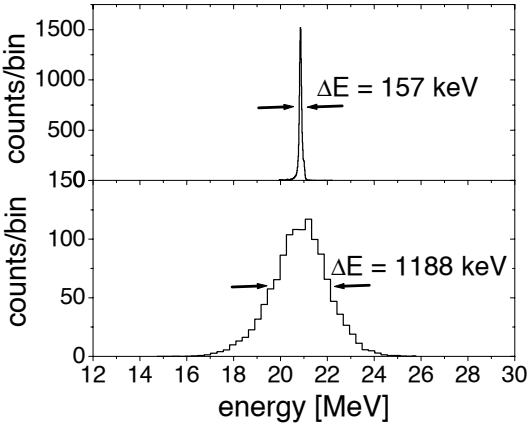

Fig. 9. Energy spectra for ^{238}U ions at $E = 20.85$ MeV taken under identical experimental conditions with an aluminum TES calorimeter *(upper part)* and a conventional silicon surface barrier detector *(lower part)*. The relative energy resolution achieved is $\Delta E/E = 7.5 \times 10^{-3}$ for the calorimetric detector, and $\Delta E/E = 57 \times 10^{-3}$ for the silicon detector, respectively.

up to about 0.5–1 kHz. The corresponding energy spectrum is displayed in Fig. 8 (right side). The solid line is the result of a fit with a Gaussian to the data resulting in a width of $\Delta E = 80$ keV, corresponding to a relative energy resolution of $\Delta E/E = 4.6 \times 10^{-3}$ which represents the best result obtained at energies below 1 MeV/amu at present. The shoulder on the low energy side is due to scattering of ions from the entrance slits.

As compared to conventional ionization detectors, the present result represents a considerable improvement in energy resolution, especially at these relatively low ion energies. For a direct comparison, a conventional silicon surface barrier detector was mounted at the same beamline (see Fig. 17) and could be moved in front of the calorimetric detector, thus allowing measurements under practically identical experimental conditions. The result of such a measurement for ^{238}U ions at $E = 20.85$ MeV is displayed in Fig. 9. It turns out that the relative energy resolution of the calorimetric detector of $\Delta E/E = 7.5 \times 10^{-3}$ is about one order of magnitude better than the resolution of $\Delta E/E = 57 \times 10^{-3}$ achieved with the silicon detector. Furthermore, a relatively fast decrease of the energy resolution of the silicon detector throughout several hours of measuring time was observed, most probably due to radiation damage, whereas the calorimetric detector showed no evidence of such behaviour even after irradiation with integrated ion doses as high as 10^9 ions/cm^2.

Results of a systematic study on the energy resolution obtained for all ions and energies investigated are summarized in Fig. 10 (left side). At low energies ($E < 20$ MeV), an increase of $\Delta E/E$ for α-particles and ^{13}C is observed. This behaviour may be explained by a lack of sensitivity of the present detectors due to their relatively large heat capacity, and could be improved in future by using substantially thinner absorbers as compared to $d = 330$ µm in the present setup. For energies $E \geq 20$ MeV, the relative energy resolution is

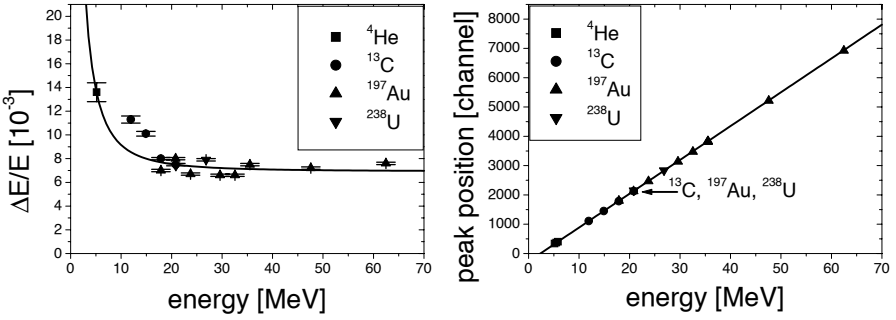

Fig. 10. Summary of a systematic study of the detector performance for various ions and energies: relative energy resolution *(left side)* and linearity of energy response *(right side)* obtained for various ions (^{4}He, ^{13}C, ^{197}Au, ^{238}U) in an energy range of $E = 5$–70 MeV. All measurements were performed with an aluminum TES calorimeter as described in Sect. 3.1.2. The *solid lines* represent fits to the data (for discussion see text).

approximately constant, independent of ion species and incident energy. The solid line is the result of a fit to the data using the ansatz:

$$\frac{\Delta E}{E} = \frac{1}{E}\sqrt{\Delta E_{BLN}^2 + (\beta E)^2} \tag{1}$$

Hereby, ΔE_{BLN} represents the contribution of the baseline noise which is supposed to limit the signal-to-noise-ratio for low energies and describes the increase in relative energy resolution for $E < 20$ MeV. For the higher energies, the term $\Delta E \sim E$ dominates, β being a proportional constant. This term is most probably due to intrinsic detector properties. It can, e.g., be caused by a position dependence of the detector response function due to incomplete thermalization of the whole absorber [27]. Further detailed investigation of the energy deposition processes will be necessary for a full understanding of the obtained detector performance.

Figure 10 (right side) summarizes the results on the linearity of the detector response. A perfectly linear behaviour as a function of energy was obtained over the entire range of ions from ^{4}He to ^{238}U. The solid line represents a linear fit to the data. Even more remarkable, the peak positions for the three different ions ^{13}C, ^{197}Au, ^{238}U at the same energy agree within 0.1%, showing no evidence of a pulse height defect. In contrast, for the conventional silicon detector a considerable pulse height defect of 70% was observed when comparing the peak position of ^{13}C to that of ^{238}U [15]. Besides the good energy resolution, we consider the non-existence of a pulse height defect for calorimetric detectors to be a considerable advantage over ionization detectors, important for many applications (see Sect. 4). Furthermore, this result allows to set an upper limit on the existence of Z-dependent energy

loss processes, like creation of Frenkel pairs etc. (see Sect. 2), and on their contribution to the energy resolution.

4 Applications of Calorimetric Low Temperature Detectors for Heavy Ions and First Results

Based on the excellent results already obtained for the performance of cryogenic heavy ion detectors (see previous section), such detectors bear the potential to be powerful tools for heavy ion physics. In the following, a brief overview of applications, including a few selected examples where also first results were obtained, is presented.

4.1 High Resolution Nuclear Spectroscopy

The investigation of direct reactions, such as elastic and inelastic scattering, few-nucleon transfer reactions, charge exchange reactions, etc., is a well known tool in nuclear physics to obtain information on nuclear structure [4]. Heavy ion detectors, which detect the scattered particles or the reaction products after the nucleus–nucleus interaction, need to have sufficient energy resolution to separate elastic from inelastic reaction channels, or to identify specific reaction channels. The availability of high-quality heavy ion beams, cooled in storage rings to highest phase space densities with a relative energy spread as good as $\Delta E/E \leq 10^{-4}$–10^{-6}, and of high resolution detectors opens new possibilities in that field.

As an example, a scattering experiment [23], performed with a relativistic heavy ion beam from the SIS18 synchrotron at GSI (see Fig. 1), representing the first application of a cryogenic detector in nuclear structure physics, is discussed. The excitation of the giant resonance, which is a collective vibrational mode of nucleons in nuclei [28], was investigated for the lead nucleus by separating inelastically from elastically scattered ions in the spectrum for scattering of 100 MeV/amu ^{20}Ne ions from a lead target. Since a beam

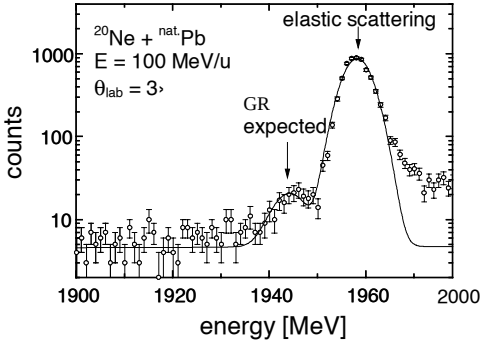

Fig. 11. Energy spectrum obtained with an aluminum TES calorimeter for scattering of a 100 MeV/amu ^{20}Ne beam from a lead target. The bump due to the excitation of the giant resonance in lead is indicated by the *label GR*. The *solid line* represents the result of Gaussian fits to the data.

particle which has excited a giant resonance in a target nucleus essentially loses an amount of kinetic energy corresponding to the excitation energy, the excitation of the resonance can be detected in the total energy spectrum of the scattered ^{20}Ne projectiles. In contrast to standard detection techniques [28], where all decay products of the giant resonance have to be detected for a missing-mass reconstruction, thus requiring a rather extended and complicated experimental setup, the present method allows a relatively simple setup, but requires high energy resolution. In Fig. 11 the measured energy spectrum for ^{20}Ne ions, scattered from a lead target at a scattering angle of $\Theta_{lab} = 3°$, is displayed. Below the elastic peak, a bump appears which is attributed to the excitation of the giant dipole resonance in the lead nuclei. The positions and the intensities of the two peaks were extracted by Gaussian fits. The resulting excitation probability of 1.7(3)% and excitation energy of 14.0(1.2) MeV are within errors in good agreement with theoretical predictions (for details see [23]).

In future it is planned to continue such investigations, the excitation of single giant resonances of different multipolarities, and especially of higher order modes, so-called multiphonon giant resonances, being of particular interest [29,30].

4.2 High Resolution Mass Determination for Identification of Superheavy Elements and Reaction Products from Direct Reactions with Radioactive Beams

The direct in-flight mass determination of nuclides produced in heavy-ion induced reactions is an important task, required in many fields of heavy ion physics, and is in many cases mandatory for a unique identification of rare isotopes and an unambiguous interpretation of experimental data. As the required relative mass resolution for resolving neighbouring masses scales with the nuclear mass M according to $1/M$, such a task turns out to be most challenging for the heaviest particle-stable isotopes under investigation.

Due to their excellent energy resolution and energy linearity because of the absence of a pulse height defect (see Sect. 3.2) and their radiation hardness, calorimetric low temperature detectors may in future be favourably used for such purposes. The idea is to replace the standard $B\rho$/TOF method, where an isotope mass $M = p/v$ is determined by a magnetic rigidity ($B\rho$) measurement of the momentum p and a **T**ime-**O**f-**F**light (TOF) measurement of the velocity v, by an energy/TOF determination of the mass via $M = 2E/v^2$. The advantage of this method is that ambiguities due to multiple charge states, as appearing in the $B\rho$/TOF method for not fully stripped ions, do not exist, and moreover, no solid angle limiting magnetic spectrometers are needed. However, since mass resolution for E/TOF measurements is determined by $\Delta M/M = [(\Delta E/E)^2 + 2(\Delta v/v)^2]^{1/2}$, it is obvious that the separation of masses up to the heaviest isotopes ($M \approx 300$ amu) will require a relative energy resolution of at least $\Delta E/E \leq 3 \times 10^{-3}$, presently obtainable

only with calorimetric low temperature detectors. The determination of the ion velocity with a relative resolution of the order of $\Delta v/v \leq 1 \times 10^{-3}$ is possible with standard TOF techniques [25,31,39] by using fast channelplate detectors and applying, especially for the case of very slow heavy ions, ultra-thin carbon foils [32] to keep energy-loss straggling on a tolerable level.

One prominent example where such a detection system could be favourably employed in future is the research on superheavy elements. An overview of this research field and of its recent progress at GSI Darmstadt and worldwide is given in [5,6]. At GSI Darmstadt, elements with $Z = 107$–112 have been successfully synthesized and unambiguously identified within the last two decades. The elements Bh ($Z = 107$), Hs ($Z = 108$), Mt ($Z = 109$), Ds ($Z = 110$) and Rg ($Z = 111$) have already been named. As discussed in more detail in [5,6], the superheavy elements have been produced by cold fusion heavy ion reactions at relatively low incident energies around 1–5 MeV/amu, and the resulting fusion products (with energies of $E = 0.1$–1 MeV/amu) are separated in the heavy ion separator SHIP and transported to a conventional silicon semiconductor detector where the heavy isotope and its α-decays are detected time-resolved. The production cross sections are as low as 10^{-10}–10^{-13} barn, corresponding to production rates down to 1/week or even less, thus demanding for a highly efficient event characterization for each single event. For the superheavy elements with $Z \leq 112$, this was possible by identifying the complete α-decay chain leading to an already known decay chain, and therefore allowing to unambiguously identify the isotope even for one single event [5,6]. Indications of the existence of superheavy elements with $Z = 113$, 114, 116 and 118 have been reported from heavy ion research centers at Dubna, Russia [33,34] and RIKEN, Japan [35]. However, for superheavy elements with $Z > 112$, the situation is essentially different, as the isotopes produced are most likely to decay by spontaneous fission instead of feeding known α-decay chains, and therefore the identification method discussed above for $Z \leq 112$ is not applicable any more.

To overcome this problem, it was recently proposed [24] to use an E/TOF detection system (see Fig. 12) with a high resolution calorimetric detector that would allow a mass identification of the superheavy nuclide produced, and in addition a precise determination of the total kinetic energy of the fission products. In a series of test experiments [15,25] performed recently at the heavy ion separator SHIP at GSI and at the VERA facility in Vienna (see Sect. 4.3), it was demonstrated that the proposed detection scheme fulfills the requirements for a successful future application in superheavy element research. At the SHIP separator, fusion products from the reaction

$$^{58}\mathrm{Ni} + ^{102}\mathrm{Ru} \rightarrow ^{160}\mathrm{Hf}^{*} \rightarrow ^{155(156)}\mathrm{Yb} + 2\mathrm{p} + 2(3)\mathrm{n}$$

and their α-decays were detected time-resolved in an aluminum TES calorimeter (as described in Sect. 3). It turned out [15] that the dynamic range of the detector was sufficient to detect the heavy ion and its correlated α-decays, and it was possible to identify the isotopes ^{155}Yb and ^{156}Yb via their α-decay

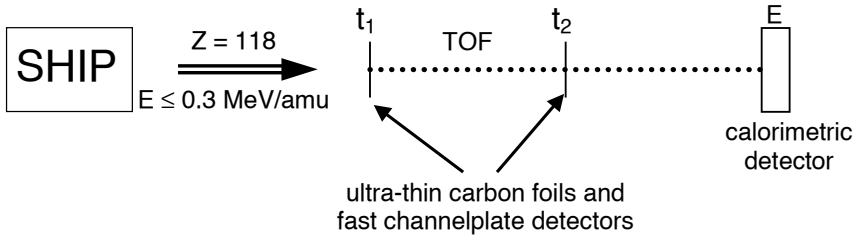

Fig. 12. Scheme of a setup proposed for the identification of superheavy elements with $Z > 112$. The mass of the superheavy nucleus, separated from other reaction products by the heavy ion separator SHIP [5], is determined by a combined E/TOF determination. Besides the superheavy nucleus, its decay products are additionally to be detected time-resolved in the calorimetric detector.

chains. The best α-resolution achieved with such detectors is $\Delta E = 32$ keV and therefore also sufficient for the demands of the proposed experiment.

In another test experiment performed at the VERA facility, direct in-flight mass identification of ^{206,208}Pb isotopes at energies slightly below 0.1 MeV/amu, close to the energy expected for superheavy elements, was tested (for details of the experimental setup see [25]). The experimental method was demonstrated to principally work, but with the not optimal energy resolution of the calorimetric detector of only $\Delta E/E = 9.8 \times 10^{-3}$ under the experimental

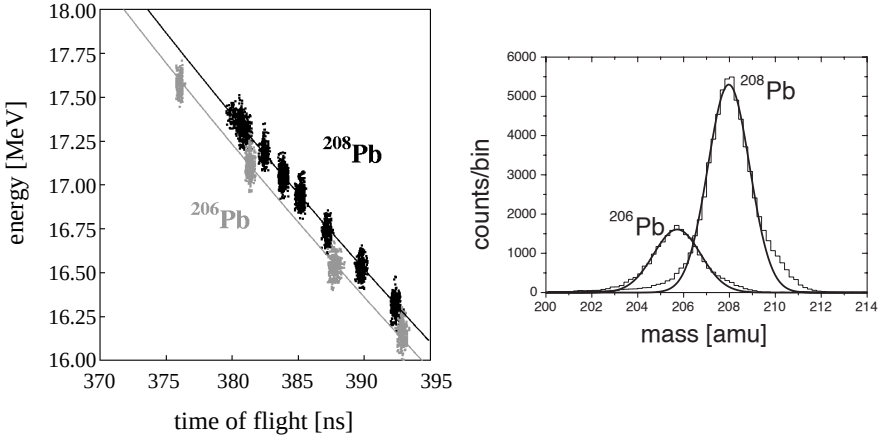

Fig. 13. Results of a test experiment for isotope identification by a combined E/TOF measurement. The energy versus time-of-flight correlation is shown on the *left side* for the isotopes ^{206}Pb and ^{208}Pb at several energies slightly below 0.1 MeV/amu. The *solid lines* represent fits to the data according to the expected kinematic correlation. The corresponding mass spectrum is displayed on the *right side*. A relative mass resolution of $\Delta M/M = 11.0 \times 10^{-3}$ is achieved.

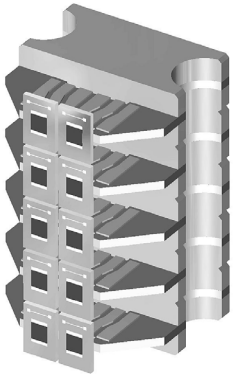

Fig. 14. Design of a prototype array consisting of 2 × 5 detector pixels of aluminum TES calorimeters.

conditions of this test run and a time resolution of $\Delta t/t = 1.4 \times 10^{-3}$, the resulting mass resolution of $\Delta M/M = 11.0 \times 10^{-3}$ allowed to separate only partly the isotopes ^{206}Pb and ^{208}Pb (see Fig. 13). With the nowadays reached energy resolution of the order of $\Delta E/E = (2-5) \times 10^{-3}$, a mass resolution of $\Delta M/M = (2-5) \times 10^{-3}$ should be achievable.

As a next step towards a cryogenic detection system for application in superheavy element research, a detector array with an active area of 3 × 8 cm^2, consisting of 96 pixels with 5 × 5 mm^2 pixel size and design values of a position resolution of $\Delta x = 5$ mm, an α-resolution of $\Delta E = 30$ keV, a heavy ion energy resolution of $\Delta E/E \leq 3 \times 10^{-3}$ and a rate capability of 300 s^{-1} per pixel is currently under design and construction. The design of a prototype array consisting of 2 × 5 detector pixels of aluminum TES calorimeters is displayed in Fig. 14.

A second example for application of cryogenic detectors to be briefly discussed concerns nuclear structure investigations on nuclei far off stability. With the availability of intense isotopically pure secondary beams of radioactive nuclei (see also Sect. 1), such investigations are most favourably performed by using the method of inverse kinematics which is sketched schematically in Fig. 15 for the example of a one-neutron (d,p) transfer reaction. In order to study the structure of the radioactive projectile nucleus, a direct reaction is initiated by the radioactive beam hitting a ^{2}H target, and the target-like reaction products are to be detected in coincidence with the beam-like reaction products. Such investigations are of high interest at present and even more at the second generation future radioactive beam facilities (see Sect. 1), as many questions of nuclear structure and nuclear astrophysics – e.g., on the isospin dependence of nuclear structure, the mechanisms of nucleosynthesis in stars and supernovae, etc. – may be addressed (see [3,4,36] for an overview).

The experimental technique (see Fig. 15) requires, among others, an unambiguous mass identification of the beam-like reaction products, which, especially for very slow heavy radioactive beams, is not provided by standard

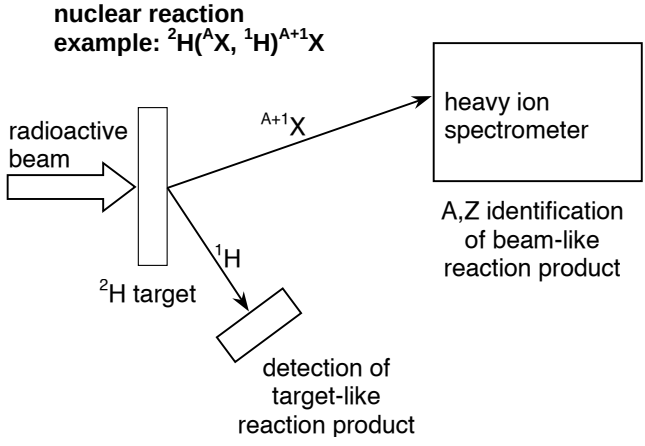

Fig. 15. Sketch of a typical experimental setup for the investigation of heavy-ion induced direct reactions with radioactive beams in inverse kinematics. For the identification of the beam-like reaction product, high resolution cryogenic detectors may favourably be used.

detection techniques. The application of cryogenic detectors for mass identification via the E/TOF method as discussed before is therefore of high interest for future investigations, e.g., at future radioactive beam facilities like SPIRAL II at GANIL, France [37], and FAIR at GSI Darmstadt, Germany [3,4].

4.3 Accelerator Mass Spectrometry

4.3.1 Cryogenic Detectors in Accelerator Mass Spectrometry

For many fields of basic and applied research in nuclear physics and astrophysics, solid state physics, material analysis, nuclear chemistry, biology, life sciences, etc., a precise knowledge of the isotopic composition of a material sample is of high interest. **A**ccelerator **M**ass **S**pectrometry (AMS) is a well established method for the determination of very small isotope ratios with high sensitivity. Preselected by a conventional "low energy" mass spectrometer, the ions of interest are injected into an accelerator. After acceleration, the ion beam passes an additional "high energy" mass spectrometer which usually consists of several filters for nuclear mass and charge, well adjustable to the individual experimental conditions for specific cases (see [7,8] for a detailed overview of the experimental technique and its applications). As compared to conventional mass spectrometry, the use of accelerated ion beams and "high energy filters" provides substantial advantage in the quality of isotope separation and suppression of background from neighbouring isotopes, isobares and molecular ions, and therefore allows an enhancement in sensitivity by

many orders of magnitude. With such performance, the precise determination of isotope ratios down to a level of 10^{-10}–10^{-16}, by far not reached with conventional techniques, becomes possible with AMS and thus enables to address interesting applications in trace analysis, radionuclide dating, cosmochronology and many others, radiocarbon dating representing the most prominent example.

Within the last 10 years, very heavy elements like uranium and plutonium have become more and more interesting for AMS applications, e.g. in biological research or reactor safety. However, AMS of such very heavy nuclides bears new and more involved challenges:

- For very heavy ions, the discrimination of neighbouring isotopes, which have always a small but finite probability to leak – due to multiple charge exchange processes – through the high energy filters, becomes more demanding. As the mass resolving power required scales linearly with the nuclear mass M, high resolution energy and/or time-of-flight detectors are necessary to separate the different isotopes.
- Most AMS facilities nowadays use tandem accelerators with 3–5 MV terminal voltage, resulting in typical ion energies as low as 0.1–1 MeV/amu for very heavy ions when selecting charge states with maximum transmission. Moreover, the present trend is to use, for cost reduction purposes, even smaller accelerators with correspondingly lower terminal voltage and thus lower ion energies. The detection of such slow heavy ions with high resolution, low threshold and high detection efficiency, most important for very rare isotopes, is a challenging task, and in many cases beyond the limits of the performance of standard detection techniques (see Sect. 2).

With the performance of cryogenic heavy ion detectors (as discussed in Sect. 3.2), such detectors have the potential to considerably improve the experimental conditions for AMS applications with very heavy ions. Due to their excellent energy resolution for slow heavy ions, they are capable of separating neighbouring masses by their high energy resolving power alone, and are therefore very suitable to replace conventional E/TOF detection systems in AMS measurements. Together with their low detection threshold and their radiation hardness, this leads to substantially improved detection efficiency and long-time stability, especially important for the detection of very rare isotopes. Consequently, as discussed in the next section, cryogenic heavy ion detectors were recently applied for the first time in an AMS experiment addressing a question of basic physics interest [15,38].

4.3.2 First Application of Cryogenic Detectors in AMS for Trace Analysis of ^{236}U

One of the heaviest nuclides of interest for AMS is ^{236}U. Being produced in nature by the capture of thermal neutrons in the reaction ^{235}U(n,γ)^{236}U and

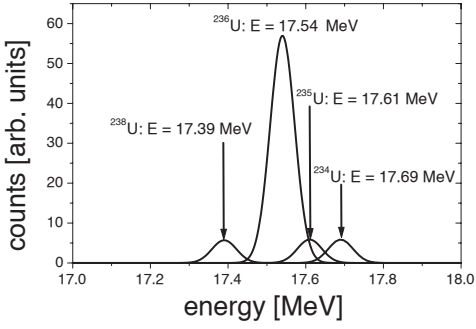

Fig. 16. Simulation of the background situation for the AMS measurement of ^{236}U. The ratio of ^{236}U:^{234,235,238}U is assumed to be 10:1, the energy resolution to be $\Delta E/E = 4.6 \times 10^{-3}$.

having a half-life of 23.4 million years, the relative abundance of ^{236}U provides an excellent neutron flux monitor integrated over geological timescales [26,39]. Besides other applications, e.g., in reactor safety, ^{236}U is therefore most interesting for geology research. Its isotopic ratio with respect to the long lived isotope ^{238}U can be used to determine the neutron flux that samples of natural uranium ore have been exposed to in their geological history. This could be used to prove the existence of an enhanced neutron flux due to natural "reactor-like" conditions in the past. A prominent example is the uranium mine in Oklo, West Africa [40], where nuclear fission of ^{235}U is believed to have occured under specific geological conditions. However, in natural uranium ore, the isotope ratio is of the order of $^{236}\mathrm{U}/^{238}\mathrm{U} = 10^{-10} - 10^{-14}$, depending on the samples history and surroundings, and therefore an ultra-high sensitivity for the detection of ^{236}U is required for such kind of investigations.

Under typical experimental conditions, e.g., at the VERA AMS facility at the university of Vienna, Austria, background in AMS measurements for very heavy ions is mainly due to neighbouring isotopes which have, due to various charge exchange processes, the same magnetic rigidity ME/q^2 (M being the mass and q the charge state of the ion) and therefore pass through the "high energy" magnetic analyzer and, after additional charge exchange, also through the electrostatic analyzer (see [26] for a detailed discussion). The background situation expected for the case of 17.54 MeV $^{236}\mathrm{U}^{5+}$ ions is displayed in Fig. 16. Since standard energy detectors, (e.g., ionization chambers etc.) do not provide sufficient energy resolution to resolve these background peaks, in the previous measurements [26,39] TOF spectrometers combined with ionization chambers were used. The level of sensitivity reached for the $^{236}\mathrm{U}/^{238}\mathrm{U}$ ratio was limited to 6×10^{-11}, mainly due to the limited detection efficiency of only 20% and/or the poor energy resolution of the ionization chamber. The aim of the present experiment was therefore to replace the conventional detection system by a calorimetric low temperature detector to increase the sensitivity, and to precisely determine the $^{236}\mathrm{U}/^{238}\mathrm{U}$ ratio for various samples of natural uranium in order to establish an improved material standard.

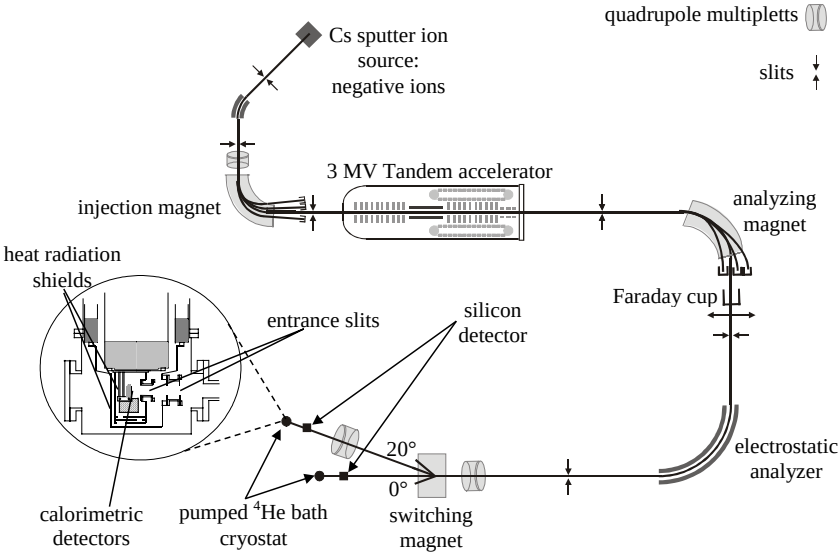

Fig. 17. The experimental setup for the AMS experiment at the Vienna Environmental Research Accelerator VERA. For the systematic investigations of detector performance discussed in Sect. 3.2, the superconducting aluminum TES calorimeters were mounted at the 0°-beamline, for the AMS measurements at the 20°-beamline. For a detailed discussion see text and [15,25,38].

The experiment was performed at the **V**ienna **E**nvironmental **R**esearch **A**ccelerator (VERA) in Vienna, Austria. This 3 MV tandem accelerator is part of a dedicated AMS setup for all ions ranging from beryllium up to uranium [26]. The experimental setup is schematically displayed in Fig. 17 (see [15,38] for details). For the AMS measurements, the accelerator provides U^{5+} beams with E $\approx$ 17.5 MeV. The analyzing magnet and the electrostatic analyzer form a high energy mass spectrometer with a mass resolution of $\Delta M/M = 1.8 \times 10^{-3}$, principally sufficient to separate ^{236}U from its neighbouring isotopes ^{234}U, ^{235}U and ^{238}U. However, due to multiple charge exchange processes with the residual gas in the beamline (as discussed above), these isotopes can pass the mass spectrometer and reach the detector at the end of the beamline, where the ^{236}U ions are detected. The cryostat which houses the aluminum TES calorimeters as described in Sect. 3.1 was attached directly to the VERA 20°-beamline. For the determination of the isotope ratio, the radioisotope ^{236}U was detected in the calorimetric detector, while the beam current of the "stable" ^{238}U was measured in a Faraday Cup situated directly behind the analyzing magnet, which was moved in and out of the beam frequently throughout the measuring cycles. Cooled slits at the entrance of the cryostat were used to minimize thermal irradiation from the

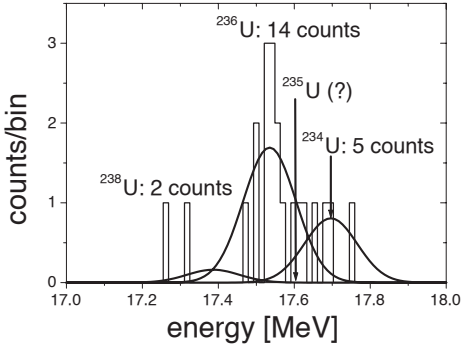

Fig. 18. Energy spectrum obtained with the aluminum TES calorimeter for the AMS measurement of the $^{236}U/^{238}U$ isotope ratio in a sample from natural uranium. The isotope ratio was determined to be $^{236}U/^{238}U = (6.1 \pm 2.1) \times 10^{-12}$.

surroundings. Typical count rates ranged from 10 s^{-1} down to 10^{-2} s^{-1} for the sample with the lowest ^{236}U abundance.

For the very first AMS measurement performed with a cryogenic detector, the results of which are presented here, the detector performance under running conditions was unfortunately worse as compared to the results presented in Sect. 3.2, but already with a resolution of $\Delta E/E = 9.1 \times 10^{-3}$, essential parts of the background from ^{234}U and ^{238}U could be separated, whereas a possible contribution of ^{235}U is still included in the ^{236}U count rate (see also Fig. 18). Several samples of natural uranium were investigated (see [15,38] for a detailed discussion). Uranium ore from the mine "Joachimsthal", processed and stored before 1918 and therefore not contaminated by nuclear bomb fallout, is very suitable as a material standard in AMS if its $^{236}U/^{238}U$ isotope ratio is known precisely. Within errors, the present result of $^{236}U/^{238}U = (3.89 \pm 0.35) \times 10^{-11}$ is in agreement with previous measurements [39]. Statistical as well as systematical errors were considerably reduced, mainly due to an improvement in detection efficiency from 20% to 65%.

With the increase in sensitivity obtained, it was possible for the first time to investigate one sample of uranium extracted from spring water from Bad Gastein, Austria, for which an isotope ratio of $^{236}U/^{238}U \leq 10^{-12}$ was expected. Fig. 18 shows the energy spectrum obtained. Due to the rather complicated sample preparation and the low uranium concentration in the water, the amount of sample material was limited, and only one measurement of 20 minutes duration could be performed. The isotope ratio was determined to be $^{236}U/^{238}U = (6.1 \pm 2.1) \times 10^{-12}$. This represents the smallest isotope ratio determined for $^{236}U/^{238}U$ up to now. As compared to the measurements with a conventional setup [39], sensitivity was enhanced by one order of magnitude. Increasing the active detector area and realizing the best resolution achieved under AMS experiment conditions (see Sect. 3.2) will allow to further increase the sensitivity and to measure even smaller isotope ratios.

5 Cryogenic Detectors for Hard X-rays and their Application in Atomic Physics with Highly Charged Heavy Ions

Besides the detection of heavy ions, the concept of cryogenic detectors also provides considerable advantage for X-ray spectroscopy in heavy ion physics. Whereas the worldwide activities on cryogenic heavy ion detectors are still very scarce, a lot of activities with various motivations and potential applications for X-ray detectors exist [16,41]. Most of these developments are restricted to the energy range $E_\gamma \leq 10$ keV. However, relativistic heavy ion beams, available e.g., at GSI Darmstadt (see Sect. 1), allow to prepare highly stripped ion beams of very heavy ions with correspondingly high electronic transition energies of the order of $E_\gamma = 50$–100 keV. Consequently, there is a demand for high resolution detectors for such "hard" X-rays.

5.1 Lamb Shift Measurements on Hydrogen-like Heavy Ions

About fifty years ago, it became evident that for small distances between electric charges the classical Coulomb interaction potential is not completely correct. The accurate experimental test of the theoretical predictions of quantum electrodynamics (QED), then developed, on corrections to the classical Coulomb interaction is still – at least for high-Z systems – one of the outstanding and most challenging problems of atomic physics. In the hydrogen atom, or in hydrogen-like ions, the QED corrections give rise to the so-called Lamb shift, which is a small deviation of the binding energies from those predicted by the relativistic Dirac-Coulomb theory (see Fig. 19). Whereas in light systems, where QED predictions were confirmed to high accuracy [42] and the higher-order contributions are almost negligible, they increase strongly with higher Z. On the other hand, the theoretical predictions of QED, which are usually performed in series expansions in $Z\alpha$ (α being the fine structure constant), become most critical for the heaviest systems, where $Z\alpha$ approaches values close to unity. Therefore, an accurate determination of the Lamb shift in hydrogen-like very heavy ions represents one of the most sensitive tests of QED in strong electromagnetic fields, not accessible otherwise [10,43,44].

The level scheme of the hydrogen-like U^{91+} ion is displayed in Fig. 19. The binding energy of the 1s-energy level is about –132 keV, thus yielding transition energies for the Lyman-α lines of about 100 keV. The 1s Lamb shift is predicted to be about 466 eV [45]. Besides the QED contributions of self energy ($\approx 80\%$) and vacuum polarization ($\approx 20\%$), the effect of finite nuclear size ($\approx 40\%$) also contributes considerably to this value. Therefore, apart from the experimental uncertainities, the accuracy on the QED test will be finally limited by the uncertainities on the finite nuclear size effects, estimated for ^{238}U to be about 0.1 eV [44,45]. This provides the Lamb shift experiments also with the potential to deduce nuclear charge radii by testing QED in one

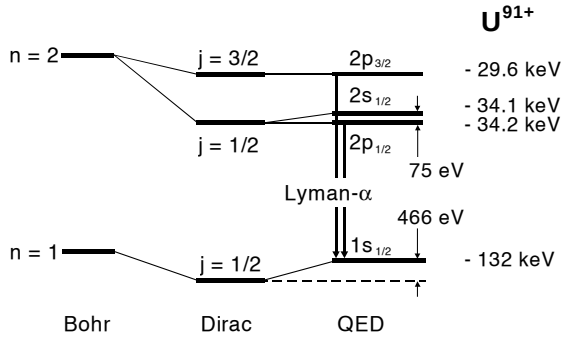

Fig. 19. Level scheme for hydrogen-like U^{91+} according to various atomic models. The numbers on the right indicate the electronic binding energies.

isotope with a well known nuclear structure, and by investigating the Lamb shift for the corresponding chain of isotopes, which may in the future also be extended to unstable isotopes.

To determine the 1s Lamb shift of heavy ions the transition energies of the Lyman-α transitions are to be measured with high accuracy and compared to theoretical predictions from the Dirac theory. Such experiments are performed at the experimental storage ring ESR of GSI Darmstadt [44,45] (see also Fig. 20). A beam of bare U^{92+} ions is injected, stored and cooled in the ESR and interacts with an internal gas-jet target. This may lead to the capture of one electron and to the population of a 2p state, which promptly decays to the 1s state. The emitted Lyman-α X-rays are detected by X-ray detectors surrounding the internal target in coincidence with the charge exchanged U^{91+} ions. The latest experimental results on the $Z = 79$ and $Z = 92$ systems are compared with theoretical predictions in [45]. The experimental results agree well with the theoretical predictions and provide already a test of QED for the high-Z domain on the level of 3%. However, the experimental errors ($\pm$ 13 eV) are about one order of magnitude larger than the theoretical ones ($\pm$ 1 eV). Thus, the experimental accuracy has to be improved considerably for a more stringent test of QED and/or for the determination of precise nuclear charge radii.

One major contribution to the experimental error is the poor energy resolution of $\Delta E \geq 500$ eV obtained with germanium detectors, which must be improved to at least $\Delta E \leq 50$–100 eV in order to reach an absolute accuracy of about $\delta E = \pm 1$ eV in the determination of the center of gravity of the transition energy. Consequently, it was first proposed in 1995 [46] to apply the concept of calorimetric low temperature detectors for improving the experimental conditions in Lamb shift experiments. As compared to the alternative concept of using crystal spectrometers [47], which also provide excellent energy resolution but suffer from poor overall detection efficiency, cryogenic detectors represent a good compromise between good energy resolution and still reasonable detection efficiency (for details see [46]). Very recently it was

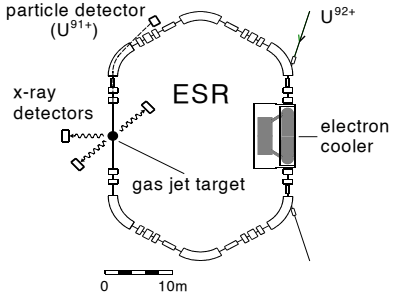

Fig. 20. Experimental setup for Lamb shift measurements on hydrogen-like very heavy ions at the internal gas-jet target of the storage ring ESR at GSI Darmstadt.

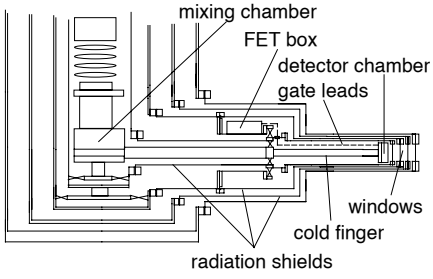

Fig. 21. Layout of the detector side arm of the ^{3}He/^{4}He delution refrigerator specially designed for the Lamb shift experiment (for details see text).

also proposed [48] to study the 2s Lamb shift in the Balmer series using calorimetric detectors covering the lower energy range of $E_\gamma \leq 10$ keV.

5.2 Development of Calorimetric Low Temperature Detectors for Hard X-rays and First Results

The detection of X-rays with calorimetric low temperature detectors is discussed in detail in the contribution of *Porter et al.* [41] for the region of soft X-rays with $E_\gamma \leq 10$ keV. To meet the experimental conditions required by the 1s Lamb shift experiment discussed in the previous section, the calorimetric detector should have a relative energy resolution of $\Delta E/E \leq 1 \times 10^{-3}$ for $E_\gamma = 50$–100 keV and a total detection efficiency (including detector solid angle) of $\geq 10^{-6}$–10^{-5}, which may be reached with a photopeak efficiency of ≥ 30 % and an active detector area of ≥ 50 mm^2. The detector modules for the present experiment are designed on the basis of silicon microcalorimeters which were developed by the Goddard / Wisconsin groups for astrophysical applications [41,49]. The detector pixels consist of silicon thermistors, made from a wafer of silicon containing an implanted thermistor and of X-ray absorbers glued on the top of the thermistors by means of an epoxy varnish. Thermistor arrays [49], consisting of 36 pixels each, are provided from the collaborating group from the Goddard Space Flight Center.

For the Lamb shift measurement, the experimental setup was optimized with respect to energy resolution and detection efficiency for hard X-rays at the experimental area of the storage ring ESR (for details see [50–52]). The final detector concept foresees three calorimeter arrays, the active area of one pixel being about 0.5 mm^2. In order to reach sufficient photopeak efficiency, the absorber should be a high-Z material and have a volume of at least $V \geq 0.5$ mm^2 $\times$ 40 μm. Additional requirements are low heat capacity as well as rapid and complete thermalization. Absorber materials under

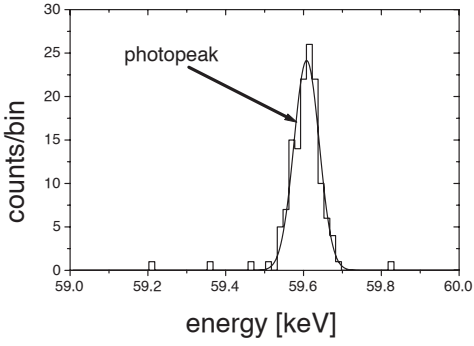

Fig. 22. Energy spectrum observed with a calorimetric low temperature detector with a 0.2 mm^2 × 47 μm Pb absorber for 59.6 keV photons. The solid line represents a Gaussian fit to the data. For the photopeak, an energy resolution of $\Delta E = 65$ eV is obtained.

investigation are Sn, HgTe and Pb. To obtain a reasonable detection solid angle, the detector arrays have to be located as close as possible to the interaction zone at the internal target of the ESR. To realize this concept a special ^{3}He/^{4}He dilution refrigerator with a side arm which fits to the internal target geometry was designed in cooperation with Oxford Instruments. A schematic view of the layout of the system is displayed in Fig. 21. The detector arrays are mounted on the cold finger at the end of the side arm and can be irradiated through a system of aluminum-coated mylar windows. In order to suppress low-frequency microphonics, the first amplifier stage is positioned close to the detectors inside the side arm of the cryostat. The cryostat is prepared to read out a total of 100 detector channels. In agreement with the specifications, the cryostat reaches a base temperature of 11.5 mK, and a cooling power of 400 μW at 11.5 mK. The operating temperature of the detectors can be chosen between T= 50 mK and T = 100 mK.

The detector performance presently achieved is already close to fulfill the demands of the Lamb shift experiment. The best results were obtained with Sn and Pb as absorber materials. The energy spectrum obtained for a detector with a 0.2 mm^2 × 47 μm Pb absorber for 59.6 keV photons, provided by an ^{241}Am source, is displayed in Fig. 22. For the photopeak at 59.6 keV, an energy resolution of $\Delta E = 65$ eV is obtained. This result may be compared to the theoretical limit of the energy resolution for a conventional semiconductor detector which is about $\Delta E \approx 380$ eV for 60 keV photons.

Very recently, a prototype array consisting of 8 pixels with a total active area of 2.9 mm^2 was installed at the ESR storage ring and is presently subject to tests under realistic experimental conditions. Covering a total solid angle of 1.9×10^{-5} sr, an overall K_α detection efficiency of 2×10^{-7}, corresponding to a count rate of 15/hour under realistic experimental conditions is expected, and an average energy resolution of $\Delta E = 75$–150 keV is obtained.

With respect to atomic physics investigations at the future GSI facility FAIR (see Sect. 1), we expect that the concept of cryogenic detectors will play a major role for X-ray spectroscopy on stored and trapped heavy ions. So within the SPARC project [53], it was proposed to build up highly efficient

arrays of calorimetric detectors covering a major part of the available solid angle. For this purpose, besides micro-calorimeters on the basis of semiconductor thermistors or transition edge sensors, as used nowadays, the concept of magnetic calorimeters [54] may be a promising detector concept for such investigations.

Acknowledgements

The authors are indepted to D. Ackermann, R. Golser, W. Henning, F. P. Hessberger, S. Hofmann, H.-J. Kluge, W. Kutschera, D. Mc Cammon, G. Münzenberg, H. J. Meier, K. W. Shepard, C. K. Stahle, P. Steier and T. Stöhlker for many helpful and stimulating discussions. The experimental results presented in this article were obtained in close collaboration with V. A. Andrianov, A. Bleile, W. Böhmer, R. Golser, W. Henning, A. v. Kienlin, A. Kiseleva, O. Kiselev, G. Kraus, W. Kutschera, U. Liebisch, H. J. Meier, J. P. Meier, A. Priller, O. Sebastian, A. Shrivastava, P. Steier, C. Vockenhuber, M. Weber and A. Weinbach.

References

1. Proceedings of the 10th International Workshop on Low Temperature Detectors LTD10, F. Gatti (ed.), Nucl. Instr. Meth. A **520** (2004)
2. Cryogenic Particle Detection, C. Enss (ed.), Topics Appl. Phys. **99** (2005)
3. W. F. Henning, Nucl. Instr. Meth. B **214**, 211 (2004)
4. Conceptual Design Report: An international accelerator facility for beams of ions and antiprotons, H. H. Gutbrod et al. (eds.), GSI Darmstadt, Germany (2001), http://www.gsi.de/zukunftsprojekt/veroeffentlichungen_e.html
5. S. Hofmann and G. Münzenberg, Rev. Mod. Phys. **72**, 733 (2000)
6. S. Hofmann, J. Nucl. Rad. Sc. **4**, R1 (2003)
7. W. Kutschera and M. Paul, Ann. Rev. Nucl. Part. Sci. **40**, 411 (1990)
8. W. Kutschera in Experimental Nuclear Physics in Europe, ENPE 99: Facing the Next Millenium, B. Rubio et al. (eds.), AIP Conference Proceedings **495**, 407 (1999)
9. Atomic Physics with Heavy Ions, H. F. Beyer, V. P. Shevelko (eds.), Springer, Berlin (1999)
10. T. Stöhlker, Physica Scripta T **73**, 29 (1997)
11. J. F. Ziegler, J. P. Biersack and U. Litmark: The stopping and range of ions in solids, Pergamon Press, New York (1985)
12. S. H. Moseley and J. C. Mather, J. Appl. Phys. **56**, 1257 (1984)
13. D. Mc Cammon in Cryogenic Particle Detection, C. Enss (ed.), Topics Appl. Phys. **99**, 1 (2005)
14. H. H. Andersen, Nucl. Instr. Meth. B **15**, 722 (1986)
15. S. Kraft-Bermuth, PhD thesis, Johannes Gutenberg Universität, Mainz (2004)
16. K. D. Irwin and G. C. Hilton in Cryogenic Particle Detection, C. Enss (ed.), Topics Appl. Phys. **99**, 63 (2005)

17. D. Mc Cammon in Cryogenic Particle Detection, C. Enss (ed.), Topics Appl. Phys. **99**, 35 (2005)
18. A. v. Kienlin, PhD thesis, Johannes Gutenberg Universität, Mainz (1993)
19. A. v. Kienlin, F. Azgui, W. Böhmer, K. Djotni, P. Egelhof, W. Henning, G. Kraus, J. Meier and K. W. Shepard, Nucl. Instr. Meth. A **368**, 815 (1996)
20. J. Meier, P. Egelhof, C. Fischer, A. Himmler, G. Kirchner, A. v. Kienlin, G. Kraus, W. Henning and K. W. Shepard, J. Low Temp. Phys. **93**, 231 (1993)
21. J. Meier, PhD thesis, Johannes Gutenberg Universität, Mainz (1994)
22. J. Meier, L. Chulkov, P. Egelhof, C. Fischer, W. Henning, A. v. Kienlin, G. Kirchner, G. Kraus and A. Weinbach, Nucl. Instr. Meth. A **370**, 259 (1996)
23. H. J. Meier, P. Egelhof, W. Henning, A. v. Kienlin, G. Kraus and A. Weinbach, Nucl. Phys. A **626**, 451c (1997)
24. P. Egelhof, Advances in Solid State Physics **39**, 61 (1999)
25. S. Kraft, A. Bleile, P. Egelhof, R. Golser, O. Kisselev, W. Kutschera, V. Liechtenstein, H. J. Meier, A. Priller, A. Shrivastava, P. Steier, C. Vockenhuber and M. Weber in Low Temperature Detectors, F.S. Porter et al. (eds.), AIP Conference Proceedings **605**, 405 (2002)
26. C. Vockenhuber, I. Ahmad, R. Golser, W. Kutschera, V. Liechtenstein, A. Priller, P. Steier and S. Winkler, Int. J. Mass. Spectr. **223-224**, 713 (2003)
27. V. A. Andrianov, A. Bleile, P. Egelhof, S. Kraft, A. Kiseleva, O. Kiselev, H. J. Meier and J. P. Meier, Nucl. Instr. Meth. A **520**, 84 (2004)
28. M. N. Harakeh and A. van der Woude: Giant Resonances, Clarendon Press, Oxford (2001)
29. T. Aumann, P. F. Bortignon and H. Emling, Annu. Rev. Nucl. Part. Sci. **48**, 351 (1998)
30. H. Emling, Prog. Part. Nucl. Phys. **33**, 729 (1994)
31. W. H. Trzaska, V. Lyapin, T. Alanko, M. Mutterer, J. Räisänen, G. Tjurin and M. Wojdyr, Nucl. Instr. Meth. B **195**, 147 (2002)
32. V. K. Liechtenstein, T. M. Ivkova, E. D. Olshanski, R. Repnow, J. Levin, R. Hellborg, P. Persson and T. Schenkel, Nucl. Instr. Meth. A **480**, 185 (2002)
33. Y. T. Oganessian, V. K. Utynkov, Y. V. Lobanov, F. S. Abdullin, A. N. Polyakov, I. V. Shirokovsky, Y. T. Tsyganov, G. G. Gulbekian, S. L. Bogomolov, B. N. Gikal, A. N. Mezentsev, S. Iliev, V. G. Subbotin, A. M. Sukhov, A. A. Voinov, G. V. Buklanov, K. Subotic, M. G. Itkis, K. J. Moody, J. F. Wild, N. J. Stoyer, M. A. Stoyer, R. W. Lougheed, C. A. Laue, J. B. Patin, D. A. Shaughnessy and J. M. Keneally in Proceedings of the Fourth Tegernsee International Conference on Particle Physics Beyond the Standard Model, BEYOND 2003, H.-V. Klapdor-Kleingrothaus (ed.), Springer, Berlin, 1091 (2004)
34. Y. T. Oganessian, V. K. Utynkov, Y. V. Lobanov, F. S. Abdullin, A. N. Polyakov, I. V. Shirokovsky, Y. T. Tsyganov, G. G. Gulbekian, S. L. Bogomolov, B. N. Gikal, A. N. Mezentsev, S. Iliev, V. G. Subbotin, A. M. Sukhov, A. A. Voinov, G. V. Buklanov, K. Subotic, V. I. Zagrebaev, M. G. Itkis, J. B. Patin, K. J. Moody, J. F. Wild, M. A. Stoyer, N. J. Stoyer, D. A. Shaughnessy, J. M. Keneally and R. W. Lougheed, Phys. Rev. C **69**, 054607 (2004)
35. K. Morita, K. Morimoto, D. Kaji, T. Akiyama, S. Goto, H. Haba, E. Ideguchi, R. Kanungo, K. Katori, H. Koura, H. Kudo, T. Ohnshi, A. Ozawa, T. Suda, K. Sueki, H. Xu, T. Yamaguchi, A. Yoneda, A. Yoshida and Y. Zhao, J. Phys. Soc. Jpn. **73**, 2593 (2004)
36. P. Egelhof, O. Kisselev, G. Münzenberg, S. R. Neumaier and H. Weick, Physica Scripta **T104**, 151 (2003)

37. http://www.ganil.fr/spiral/
38. S. Kraft, V. Andrianov, A. Bleile, P. Egelhof, R. Golser, A. Kiseleva, O. Kiselev, W. Kutschera, J. P. Meier, A. Priller, A. Shrivastava, P. Steier and C. Vockenhuber, Nucl. Instr. Meth. A **520**, 63 (2004)
39. P. Steier, R. Golser, W. Kutschera, A. Priller, A. Valenta, C. Vockenhuber and V. Liechtenstein, Nucl. Instr. Meth. B **188**, 283 (2002)
40. C. A. Cowen, Scientifc American **235**, 36 (1976)
41. F. S. Porter, G. V. Brown and J. Cottom in Cryogenic Particle Detection, C. Enss (ed.), Topics Appl. Phys. **99**, 361 (2005)
42. M. Weitz, F. Schmidt-Kaler and T. W. Hänsch, Phys. Rev. Lett. **68**, 1120 (1992)
43. T. Stöhlker, T. Beier, H. F. Beyer, T. Kühl and W. Quint: Tests of Strong Field QED – The Physics of Multiply and Highly Charged Ions, Kluwer Academic Publishers (2003)
44. P. M. Mohr, G. Plunien, G. Soff, Phys. Rep. **293**, 227 (1998)
45. T. Stöhlker, P. H. Mokler, F. Bosch, R. W. Dunford, F. Franzke, O. Klepper, C. Kozhuharov, T. Ludziejewski, F. Nolden, H. Reich, P. Rymuza, Z. Stachura, M. Steck, P. Swiat and A. Warczak, Phys. Rev. Lett. **85**, 3109 (2000), and references therein
46. P. Egelhof, H. F. Beyer, D. Mc Cammon, F. v. Feilitzsch, A. v. Kienlin, H.-J. Kluge, D. Liesen, J. Meier, S. H. Moseley and T. Stöhlker, Nucl. Instr. Meth. A **370**, 263 (1996)
47. H. F. Beyer, T. Stöhlker, D. Banas, D. Liesen, D. Protic, K. Beckert, P. Beller, J. Bojowald, F. Bosch, E. Förster, B. Franzke, A. Gumberidze, S. Hagmann, J. Hoszowska, P. Indelicato, O. Klepper, H.-J. Kluge, S. König, C. Kozhuharov, X. Ma, B. Manil, I. Mohos, A. Orsic-Muthig, F. Nolden, U. Popp, A. Simionovici, D. Sierpowski, U. Spillmann, Z. Stachura, M. Steck, S. Tachenov, M. Trassinelli, A. Warczak, O. Wehrhan and E. Ziegler, Spectrochimica Acta B **59**, 1535 (2004)
48. E. Silver, H. Schnopper, G. Austin, R. Ingram, G. Guth, S. Murray, N. Madden, D. Landis, J. Beeman, E. E. Haller and T. Stöhlker, Nucl. Instr. Meth. A **520**, 60 (2004)
49. C. K. Stahle, R. L. Kelley, D. Mc Cammon, S. H. Moseley and A. E. Szymkowiak, Nucl. Instr. Meth. A **370**, 173 (1996)
50. J. Meier, P. Egelhof, S. Han, H.-J. Kluge, D. Mc Cammon, T. Mihara, S. H. Moseley and C. K. Stahle in Proc. of the 7th Int. Workshop on Low Temperature Detectors LTD7, Munich, S. Cooper (ed.), MPI of Physics, Munich, 213 (1997)
51. A. Bleile, P. Egelhof, H.-J. Kluge, U. Liebisch, D. Mc Cammon, H. J. Meier, O. Sebastian, C. K. Stahle and M. Weber, Nucl. Instr. Meth. A **444**, 488 (2000)
52. A. Bleile, P. Egelhof, S. Kraft, D. Mc Cammon, H. J. Meier, A. Shrivastava, C. K. Stahle and M. Weber in Low Temperature Detectors, F.S. Porter et al. (eds.), AIP Conference Proceedings **605**, 409 (2002)
53. http://www.gsi.de/zukunftsprojekt/experimente/sparc/index_e.html
54. A. Fleischmann, C. Enss and G. M. Seidel in Cryogenic Particle Detection, C. Enss (ed.), Topics Appl. Phys. **99**, 151 (2005)